Molecular Biology of the Cell
Vol. 18, 1009–1017, March 2007

Two Regions of the Tail Are Necessary for the Isoform-specific Functions of Nonmuscle Myosin IIB[D] [V]

Masaaki K. Sato, Masayuki Takahashi, and Michio Yazawa

Division of Chemistry, Graduate School of Science, Hokkaido University, Sapporo, 060-0810 Japan

Submitted August 14, 2006; Revised December 20, 2006; Accepted December 22, 2006
Monitoring Editor: Yu-li Wang

To function in the cell, nonmuscle myosin II molecules assemble into filaments through their C-terminal tails. Because myosin II isoforms most likely assemble into homo-filaments in vivo, it seems that some self-recognition mechanisms of individual myosin II isoforms should exist. Exogenous expression of myosin IIB rod fragment is thus expected to prevent the function of myosin IIB specifically. We expected to reveal some self-recognition sites of myosin IIB from the phenotype by expressing appropriate myosin IIB rod fragments. We expressed the C-terminal 305-residue rod fragment of the myosin IIB heavy chain (BRF305) in MRC-5 SV1 TG1 cells. As a result, unstable morphology was observed like MHC-IIB$^{-/-}$ fibroblasts. This phenotype was not observed in cells expressing BRF305 mutants: 1) with a defect in assembling, 2) lacking N-terminal 57 residues (N-57), or 3) lacking C-terminal 63 residues (C-63). A myosin IIA rod fragment ARF296 corresponding to BRF305 was not effective. However, the chimeric ARF296, in which the N-57 and C-63 of BRF305 were substituted for the corresponding regions of ARF296, acquired the ability to induce unstable morphology. We propose that the N-57 and C-63 of BRF305 are involved in self-recognition when myosin IIB molecules assemble into homo-filament.

INTRODUCTION

Myosins constitute a large superfamily of actin-based molecular motors (Sellers, 1999; Berg *et al.,* 2001). Nonmuscle myosin II, one of the members of the superfamily, is involved in various cell functions such as cytokinesis (Robinson and Spudich, 2004; Matsumura, 2005) and migration (Lauffenburger and Horwitz, 1996; Mitchison and Cramer, 1996). In mammalian cells, there are three isoforms of the nonmuscle myosin II heavy chain (MHC) referred to as MHC-IIA, MHC-IIB, and MHC-IIC, which together with two pairs of light chains form myosin IIA, myosin IIB, and myosin IIC, respectively (Berg *et al.,* 2001; Golomb *et al.,* 2004).

Recently, it has been shown that each myosin II isoform has specific functions. Concerning two of the isoforms, myosin IIA and myosin IIB, the functional differences are suggested by the embryonic lethal phenotypes after their ablation in mice (Tullio *et al.,* 1997; Conti *et al.,* 2004). From the unstable morphology of MHC-IIB$^{-/-}$ cells, it was clearly demonstrated that myosin IIB is involved in the guidance of fibroblast migration by coordinating protrusive activities and stabilizing cell polarity (Lo *et al.,* 2004). Because this defect was rescued by the exogenous expression of MHC-IIB but not MHC-IIA, it is probable that the specific functions of each myosin II isoform could not be complemented by the other completely.

Myosin II functions by assembling of monomers into filaments (Craig and Woodhead, 2006). Carboxyl terminal α-helical coiled-coil rod-like tails are involved in assembly through electrostatic interaction (McLachlan, 1984), and critical regions for the assembly are located in its carboxyl-terminus (Hodge *et al.,* 1992; Sohn *et al.,* 1997; Nakasawa *et al.,* 2005). In nonmuscle cells, dynamic assembly/disassembly of myosin II molecules is organized spatiotemporally in response to various signals. To function effectively, it is reasonable to consider that they assemble in an isoform-specific mode to form homo-filaments (homogeneous with respect to their subunit composition) in the cell because of differences in their subcellular localization (Maupin *et al.,* 1994; Rochlin *et al.,* 1995; Kolega, 1998, 2003; Saitoh *et al.,* 2001) as well as their ATPase and motor activities (Kelley *et al.,* 1996; Golomb *et al.,* 2004). However, hetero-filaments were formed when their carboxyl-terminal rod fragments were mixed in vitro (Murakami *et al.,* 2000). These gave us an idea that some self-recognition mechanisms of individual myosin II isoforms might exist and result in myosin II isoforms assembling into homo-filaments in the cell.

Because filament formation is necessary for myosin II to function, exogenous expression of rod fragment containing the critical regions for assembly could exhibit a dominant negative effect to prevent the normal assembly of endogenous myosin II. In fact, it was shown that a 72-kDa rod fragment of MHC-IIB acts as a dominant-negative form and induced aberrant cell shape (Ben-Ya'acov and Ravid, 2003). This study induced us to see the effects of exogenous expression of the rod fragments of each isoform in the cell. If some sites responsible for self-recognition are found to reside in the expressed rod fragments, they would be expected to bind the corresponding myosin II isoform and inhibit the function in an isoform-specific manner. We expected to reveal the self-recognition sites of myosin IIB from the pheno-

This article was published online ahead of print in *MBC in Press* (http://www.molbiolcell.org/cgi/doi/10.1091/mbc.E06–08–0706) on January 3, 2007.

[D] [V] The online version of this article contains supplemental material at *MBC Online* (http://www.molbiolcell.org).

Address correspondence to: Masayuki Takahashi (takahash@sci.hokudai.ac.jp).

Abbreviations used: MHC, myosin heavy chain; BRF, MHC-IIB rod fragment; ARF, MHC-IIA rod fragment; nACD, nonmuscle myosin assembly competence domain.

Table 1. Primers used for mutagenic PCR

Fragment	Primer[a]
BRF305-m3	
Forward	5′-GAGCAGCTTAAAGAACAGCTGGAGGAAGCA-3′
Reverse	5′-CATCCGAGCGTTGGCCTCCTCCATCTGCTC-3′
BRF305ΔC63	
Forward	5′-TGGATGATGCCACCGAGGCCTAAGGATCCACCGGATCTAG-3′
Reverse	5′-CTAGATCCGGTGGATCCTTAGGCCTCGGTGGCATCATCCA-3′
ARF296exN	
Forward	5′-CAGATCTCGAGCTCAAGCTTTTTGC-3′
Reverse	5′-TCCAGACGCCGCTTCTCCTCCAGCAGCGCGGACTTGCCAG-3′
ARF296exC	
Forward	5′-TGGAGGACGCCACTGAGACGAACGAGGGCCTGAGCCGCGA-3′
Reverse	5′-CTAGATCCGGTGGATCCTTACTCTG-3′
BRF305exN	
Forward	5′-CAGATCTCGAGCTCAAGCTT**CTGGCCCAGGCCAAAGAGAA**-3′
Reverse	5′-TCCAGACGCCGCTTCTCATC**TAACGCCAGGGCTCCTTTGC**-3′
BRF305exC	
Forward	5′-TGGATGATGCCACCGAGGCC**GCCGATGCCATGAACCGCGA**-3′
Reverse	5′-CTAGATCCGGTGGATCCTTA**TTCGGCAGGTTTGGCCTCAG**-3′

[a] Letters with an underscore and boldface letters with an underscore indicate sequences annealing to pEGFP-BRF305 and pEGFP-ARF296 in first-step PCR, respectively.

type with aberrant cell shape by expressing appropriate myosin IIB rod fragment.

In this article, we demonstrated that the myosin IIB rod fragment, BRF305 (Phe 1672-Glu 1976), can inhibit the function of endogenous myosin IIB by inhibiting normal filament assembly. Moreover, we demonstrated that the self-recognition sites reside in the N-terminal 57 and the C-terminal 63 residues of BRF305.

MATERIALS AND METHODS

Cell Culture

MRC-5 SV1 TG1 cells, SV40-transformant of human embryonic lung fibroblast MRC-5, were obtained from RIKEN Cell Bank (Tsukuba, Japan). The cells were maintained in RITC 80-7 medium (Iwaki, Tokyo, Japan) supplemented with 10% fetal bovine serum (BioSource, Rockville, MD), 50 U/ml penicillin, and 50 μg/ml streptomycin under the condition of 37°C, humidified 5% CO_2.

Antibodies and Reagents

Anti-MHC-IIA polyclonal antibody (pAb) was produced against a synthetic peptide, Cys-Lys-Ala-Asp-Gly-Ala-Glu-Ala-Lys-Pro-Ala-Glu (carboxy terminus of human nonmuscle MHC-IIA with extra Cys at the N-terminus). Immunization and purification of the antibody were performed according to the protocol described previously (Takahashi *et al.*, 1999). Anti-MHC-IIB (C-term) pAb against carboxy terminus of MHC-IIB was described previously (Saitoh *et al.*, 2001). Anti-MHC-IIB (N-term) pAb against amino terminus of MHC-IIB was a kind gift from Dr. Robert S. Adelstein (National Heart, Lung, and Blood Institute [NHLBI], National Institutes of Health, Bethesda, MD). Anti-green fluorescent protein (GFP) mAb was purchased from Roche Applied Science (Indianapolis, IN). Anti-α-tubulin mAb and TRITC-labeled phalloidin were purchased from Sigma (St. Louis, MO). Cy3-conjugated anti-rabbit IgG antibody was purchased from Jackson ImmunoResearch Laboratories (West Groove, PA). Horseradish peroxidase–labeled anti-rabbit IgG F(ab′)2 fragment was purchased from ICN Pharmaceuticals (Aurora, OH). Horseradish peroxidase–labeled anti-mouse IgG was purchased from Bio-Rad Laboratories (Hercules, CA).

Construction of Plasmid DNA

The DNA fragment encoding Asp 1729-Glu 1976 of human nonmuscle MHC-IIB (BRF248) was amplified from a human brain cDNA library (Clontech, Mountain View, CA) as a template by PCR. The fragment was subcloned into the EcoRI-BamHI sites of pEGFP-C1 (Clontech, Mountain View, CA) to generate pEGFP-BRF248. DNA fragments encoding Leu 1666-Glu 1961 of human nonmuscle MHC-IIA (ARF296) and Phe 1672-Glu 1976 of human nonmuscle MHC-IIB (BRF305) were amplified by PCR using the plasmids pET-ARF296 and pET-BRF305 (our unpublished data) as templates. Each of them was subcloned into the HindIII-BamHI sites of pEGFP-C3 (Clontech) to generate the pEGFP-ARF296 and pEGFP-BRF305, respectively. pEGFP-BRF305-m3 and pEGFP-BRF305ΔC63 were constructed using QuikChange II XL Site-Directed Mutagenesis Kit (Stratagene, La Jolla, CA) according to the manufacturer's protocol using primer sets described in Table 1 and pEGFP-BRF305 as a template. Plasmids for expressing the chimeric rod fragments of ARF296-BRF305 were constructed by using a two-step PCR according to the method of Geiser *et al.* (2001). In brief, first PCRs were performed using pEGFP-ARF296 or pEGFP-BRF305 as templates and the appropriate mutagenic primer sets described in Table 1. The mutagenic primers were designed to anneal cDNA of one isoform with additional sequence for another. Then second PCRs were performed using the products from the first PCR as megaprimers and either pEGFP-ARF296 or pEGFP-BRF305 as a template for an inverse PCR following the QuikChange protocol. To construct pEGFP-ARF296exN and pEGFP-ARF296exC, pEGFP-ARF296 was used as a template. To construct pEGFP-BRF305exN and pEGFP-BRF305exC, pEGFP-BRF305 was used as a template. To construct pEGFP-ARF296exNC, pEGFP-ARF296exC was used as a template. The fragments produced by these plasmid DNA constructs are illustrated in Figure 1. DNA sequences were confirmed using a DNA sequencer (ABI PRISM 310; Applied Biosystems, Foster City, CA).

Transfection

Transfection was performed with Lipofectamine 2000 (Invitrogen, Carlsbad, CA) according to the manufacturer's protocol with the following modification. Cell suspension in Opti-MEM I Reduced Serum Medium (Invitrogen) was mixed with DNA-Lipofectamine 2000 complexes and then plated on a 24-well plate. After incubation for 5 h in culturing condition, cells were replated onto a 35-mm tissue culture dish (Iwaki, Tokyo, Japan) or a collagen type IC (Nitta Gelatin, Tokyo, Japan) coated coverglass. After 24 h, the transfected cells were subjected to subsequent experiments. Transfection efficiency was ~60% in all cases.

SDS-PAGE and Immunoblotting

Transfected cells were washed three times with ice-cold PBS (137 mM NaCl, 2.7 mM KCl, 8.1 mM Na_2HPO_4, 1.5 mM KH_2PO_4) and were treated with SDS lysis buffer (1% SDS, 6.25 mM Tris-HCl, pH 6.8, 10% glycerol, 10% 2-mercaptoethanol). The lysate was collected and boiled for 5 min. SDS-PAGE was performed using the buffer system of Laemmli (1970). The separated polypeptides were electrotransferred onto Immobilon-P membrane (Millipore, Billerica, MA). The membrane was preincubated with 5% skim milk and 0.1% Tween-20 in PBS for 60 min. The membrane was incubated with primary antibodies for 60 min and secondary antibody for 30 min at 23°C. The antibodies were diluted as follows: anti-GFP mAb (1:1000), anti-MHC-IIA pAb (1:10,000), anti-MHC-IIB (C-term) pAb (1:10,000), anti-α-tubulin mAb (1:10,000), horseradish peroxidase–labeled anti-mouse IgG antibody (1:20,000), and horseradish peroxidase–labeled anti-rabbit IgG antibody (1:20,000). The chemiluminescent signals were produced using ECL Plus Western blotting detection reagents (GE Healthcare, Piscataway, NJ). The signals were detected using

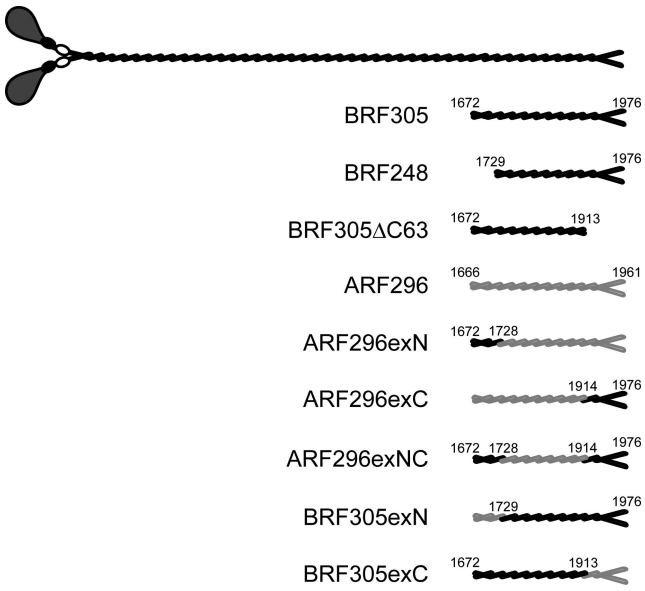

Figure 1. Schematic diagrams of myosin II rod fragments and a full-length myosin II. The myosin II rod fragments were expressed as N-terminal GFP-fused proteins. Numbers indicate amino acid residues of MHC-IIA (for ARF296) and MHC-IIB (for other fragments). Dark and light grays represent the portions derived from myosin IIB and myosin IIA, respectively.

LAS-3000 (Fujifilm, Tokyo, Japan) and analyzed by using MultiGauge version 2.2 software (Fujifilm).

Immunoprecipitation

The transfected cells were lysed with lysis buffer (30 mM NaCl, 0.1% IGEPAL CA-630, 20 mM Tris-HCl, pH 7.5, 0.1 mM PMSF, 5 μg/ml leupeptin, 2 μg/ml pepstatin A, 5 μg/ml aprotinin, 20 mM NaF, 1 mM Na_3VO_4). After centrifugation (22,000 $\times$ *g*) for 15 min at 4°C, anti-MHC-IIB (N-term) pAb was added to the supernatant, which was followed by incubation for 60 min at 4°C. The immunocomplexes were captured by protein G Sepharose beads (GE Healthcare) and then collected by centrifugation (14,000 $\times$ *g*) for 5 s. The beads were washed three times in a wash buffer (50 mM NaCl, 0.1% IGEPAL CA-630, 20 mM Tris-HCl, pH 7.5, 2 mM $MgCl_2$). For SDS-PAGE, the immunoprecipitates were eluted in 2$\times$ SDS lysis buffer with boiling for 5 min.

Immunofluorescence

In the case of staining by anti-MHC-IIB (C-term) pAb or TRITC-phalloidin, the cells cultured on a collagen (type IC)-coated coverglass were fixed with 3.7% formaldehyde in PBS for 20 min followed by permeabilization with 0.2% Triton X-100 in PBS for 5 min. The fixed cells were preincubated with 3% bovine serum albumin in PBS for 30 min. Incubation with the anti-MHC-IIB (C-term) pAb (1:1500) was carried out for 60 min. In the case of staining by anti-MHC-IIB (N-term) pAb, the cells were permeabilized in 0.5% Triton X-100 with 5% sucrose/PBS and 4% paraformaldehyde for 4 min and then fixed in 4% paraformaldehyde with 5% sucrose/PBS for 25 min. The fixed cells were preincubated with 1% bovine serum albumin in PBS for 30 min. Incubation with the anti-MHC-IIB (N-term) pAb (1:500) was carried out for 2 h. Indirect immunolabeling was performed by incubation with Cy3-labeled anti-rabbit IgG antibody (1:500) containing TRITC-labeled phalloidin (67 ng/ml) and DAPI (10 ng/ml) for 60 min. The images were captured using a conventional fluorescence microscope (BX50WI; Olympus, Tokyo, Japan), equipped with a color chilled 3CCD camera (DP70; Olympus) and an objective lens (UPlanApo 20$\times$/0.70; Olympus). All procedures were performed at 23°C.

Cell Imaging

Twenty-four hours after transfection, the images were captured using an inverted phase-contrast microscope (IX71; Olympus), equipped with a color chilled 3CCD camera (DP70; Olympus) and an objective lens (LCPlanFl 20$\times$/0.40; Olympus). For time-lapse microscopy, the images were captured every 1 min and analyzed by using Lumina Vision version 2.4.2 software (Mitani, Fukui, Japan). During observation, cells were warmed at 37°C on a thermoplate (MATS-U55R30; Tokai Hit, Shizuoka, Japan).

RESULTS

Myosin IIB Rod Fragment, BRF305, Induces the Phenotype of Unstable Cell Shape Similar to MHC-IIB$^{-/-}$ Fibroblasts

To confirm whether the exogenous expression of myosin IIB rod fragment could inhibit the function of endogenous myosin IIB in the cell, the C-terminal rod fragment of MHC-IIB consisting of the C-terminal 305 amino acid residues (BRF305) was expressed as an N-terminal GFP-fusion protein (GFP-BRF305) in MRC-5 SV1 TG1 cells. In contrast to control cells expressing GFP (Figure 2, A and B), the cells expressing GFP-BRF305 displayed aberrant shape with multiple protrusions

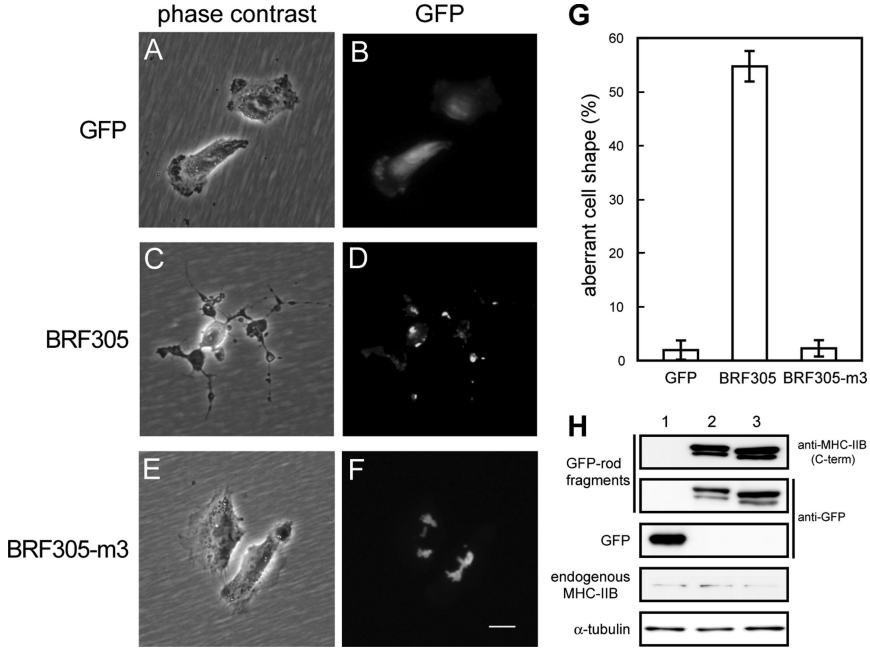

Figure 2. Expression of GFP-BRF305, but not its assembly-deficient mutant (GFP-BRF305-m3) in MRC-5 SV1 TG1 cells induced aberrant cell shape. The images were taken from live cells expressing GFP as control (A and B), GFP-BRF305 (C and D), and GFP-BRF305-m3 (E and F). Note that GFP signals were observed throughout the cytoplasm besides bright aggregates in the case of expression of GFP-fused rod fragments (D and F). Bar, 20 μm. (G) Percentage of cells with aberrant shapes seen 24 h after transfection were calculated from at least 70 cells expressing GFP fluorescence. Cells showing shrunken cell body with long protrusions or projecting multiple protrusions were regarded as "aberrant cell shape." Error bars, $\pm$SD of three independent experiments. (H) Immunoblot analyses for checking the expression levels of each exogenous protein. Lysates from the cells expressing GFP (lane 1), GFP-BRF305-m3 (lane 2), and GFP-BRF305 (lane 3) were analyzed by anti-MHC-IIB (C-term) pAb (top and forth panels), anti-GFP mAb (second and third panels), and anti-α-tubulin mAb (bottom panel). The signals of GFP-rod fragments (top panel) and endogenous MHC-IIB (forth panel) were detected simultaneously on the same immunoblot. α-tubulin was used as a loading control.

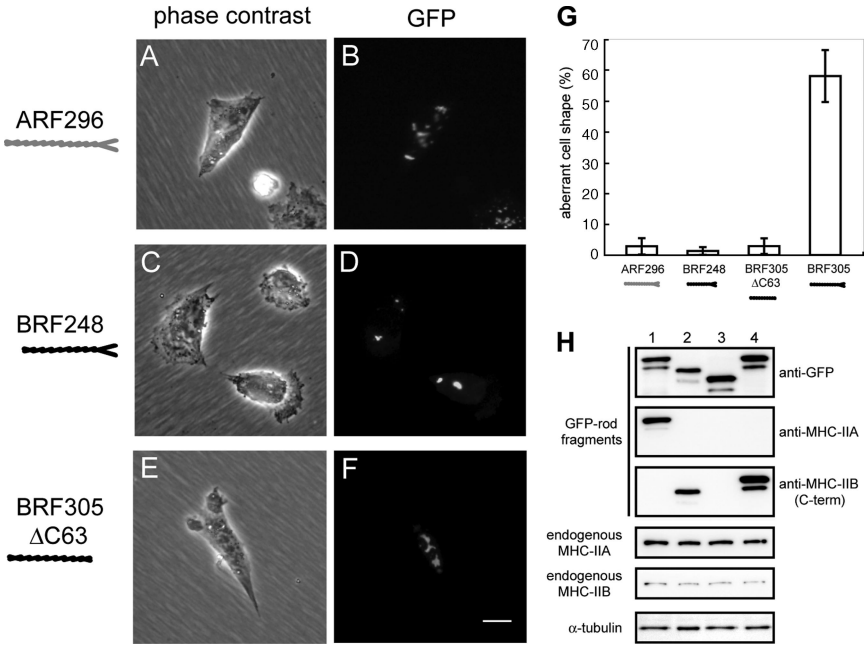

Figure 3. Aberrant cell shape was not induced by the expression of ARF296 or the deletion fragments of BRF305. The images were taken from live cells expressing GFP-ARF296 (A and B), GFP-BRF248 (C and D), and GFP-BRFΔC63 (E and F). Bar, 20 μm. (G) Percentage of cells with aberrant shapes seen 24 h after transfection were calculated from at least 70 cells expressing GFP fluorescence. Error bars, ±SD of three independent experiments. The effect of GFP-BRF305 was reconfirmed in each experiment. (H) Immunoblot analyses for checking the expression levels of each exogenous protein. Lysates from the cells expressing GFP-ARF296 (lane 1), GFP-BRF248 (lane 2), GFP-BRF305ΔC63 (lane 3), and GFP-BRF305 (lane 4) were analyzed using anti-GFP mAb (top panel), anti-MHC-IIA pAb (second and forth panels), anti-MHC-IIB (C-term) pAb (third and fifth panels), and anti-α-tubulin mAb (bottom panel). Because GFP-BRF305ΔC63 lacks a C-terminus, it was not detected by anti-MHC-IIB (C-term) pAb. The signals of GFP-rod fragments (second panel) and endogenous MHC-IIA (forth panel) were detected simultaneously on the same immunoblot. The signals of GFP-rod fragments (third panel) and endogenous MHC-IIB (fifth panel) were detected simultaneously on the same immunoblot. α-tubulin was used as a loading control.

(Figure 2, C and D) similar to the cells expressing the 72-kDa rod fragment of MHC-IIB (Ben-Ya'acov and Ravid, 2003). Time-lapse analysis revealed that the behaviors of GFP-BRF305–expressing cells were quite unstable, and disorganized protrusions were formed into all peripheral areas. The cell body moved randomly with multiple pseudopod-like structures, but faster than normal cells, and the cells seemed to have a defect in retracting the tails (Supplementary Movie 1). Approximately 55% of the cells showed this phenotype (Figure 2G). This unstable phenotype was quite similar to MHC-IIB$^{-/-}$ fibroblasts (Lo *et al.*, 2004). In spite of the unstable shape during interphase, GFP-BRF305–expressing cells rounded up during mitosis and subsequently divided into two daughter cells (Supplementary Movie 2) in a manner similar to that of control cells (Supplementary Movie 3). When the cell started to respread, it immediately displayed the unstable phenotype again. The presence of a long and thin protrusion that remained between the two daughter cells could be caused by a defect in retracting the tail that was observed in the migrating cell (Supplementary Movie 1). The unstable phenotype was not induced by the expression of GFP-BRF305-m3 (Lys1874Glu, Lys1880Glu, and Arg1884Glu), which is a mutant having a defect in assembly under physiological conditions in vitro (our unpublished data; Figure 2, E–G). The expression levels of both GFP-BRF305 and GFP-BRF305-m3 were significantly higher than that of endogenous MHC-IIB. In addition, the expression level of GFP-BRF305-m3 was comparable to that of GFP-BRF305, indicating that the lack of ability to induce the unstable phenotype is not caused by the difference of expression levels (Figure 2H). These results indicate that expression of BRF305 in the cell could inhibit the function of endogenous myosin IIB. The ability of the rod fragment to assemble is necessary for the induction of the unstable phenotype.

To see whether the exogenous expression of the myosin IIA rod fragment ARF296 corresponding to the BRF305 induces the unstable phenotype, we exogenously expressed GFP-ARF296 in the cell. GFP-ARF296 did not induce the aberrant cell shape (Figure 3, A, B, and G). The relative expression level of GFP-ARF296 was approximately three times higher than that of the endogenous MHC-IIA, as estimated from following calculation: the value 1.8, which is a ratio of signal intensity of GFP-ARF296 (Figure 3H, second panel, lane 1) to that of endogenous MHC-IIA (Figure 3H, fourth panel, lane 1), divided by the value 0.6, which is the transfection efficiency of the experiment, equals three. On the other hand, the relative expression levels of GFP-BRF305 and GFP-ARF296 against the endogenous MHC-IIB were estimated 90 times and 45 times, respectively (Supplementary Figure S1). Next, we assessed the effect of exogenous expression of the deletion mutants of BRF305 in the cell. We made deletion mutants that retained the critical regions for assembly, nACD1 and nACD2 (Nakasawa *et al.*, 2005). One is GFP-BRF248 lacking 57 residues of the N-terminal side of nACD1, another is GFP-BRF305ΔC63 lacking 63 residues of the C-terminal side of nACD2. Although GFP-BRF248 has been shown to assemble at physiological ionic conditions in vitro previously (Nakasawa *et al.*, 2005), it did not induce the aberrant cell shape (Figure 3, C, D, and G). Similarly, GFP-BRF305ΔC63 was ineffective on the cell shape (Figure 3, E–G). These results suggest that the dominant negative effect of BRF305 is caused by an isoform-specific manner and is lost by deletion of N-terminal 57 residues or C-terminal 63 residues of BRF305. In this article, we refer to the N-terminal 57 residues and C-terminal 63 residues as N-57 and C-63, respectively.

N-57 and C-63 of BRF305 Are Essential for the Isoform-specific Dominant Negative Effect

To verify the importance of the N-57 and C-63 of BRF305 for the dominant negative effect, we constructed five kinds of BRF305-ARF296 chimeric fragments (Figure 1) and analyzed their ability to induce the aberrant phenotype. All chimeric fragments showed an ability to act as dominant negative forms (Figure 4, A–J), although the degree of the effect was different from one another (Figure 4K). The abilities of both BRF305exC and BRF305exN were decreased from that of original BRF305. BRF305exC showed a more notable decrease than BRF305exN did. In contrast, the abilities of both

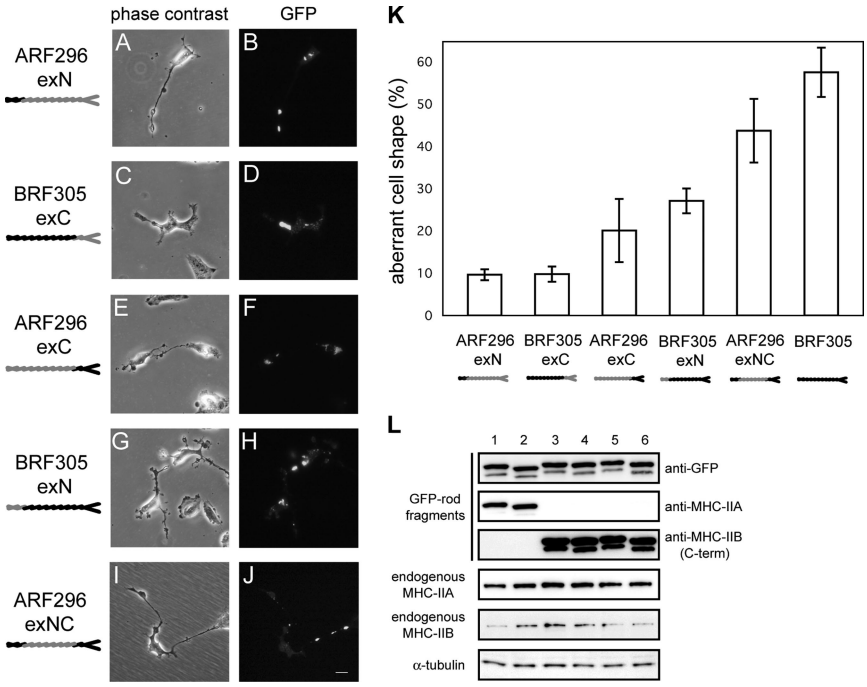

Figure 4. Induction of aberrant cell shape by the expression of BRF305-ARF296 chimeric fragments. The images were taken from live cells expressing GFP-ARF296exN (A and B), GFP-BRF305exC (C and D), GFP-ARF296exC (E and F), GFP-BRF305exN (G and H), and GFP-ARF296exNC (I and J). Bar, 20 μm. (K) Percentage of cells with aberrant shapes seen 24 h after transfection were calculated from at least 70 cells expressing GFP fluorescence. Error bars, ±SD of three independent experiments. The morphological scoring of cells was performed in a double-blind manner. The effect of GFP-BRF305 was reconfirmed in each experiment. (L) Immunoblot analyses for checking the expression levels of each exogenous protein. Lysates from the cells expressing GFP-ARF296exN (lane 1), GFP-BRF305exC (lane 2), GFP-ARF296exC (lane 3), GFP-BRF305exN (lane 4), GFP-ARF296exNC (lane 5), and GFP-BRF305 (lane 6) were analyzed by anti-GFP mAb (top panel), anti-MHC-IIA pAb (second and forth panels), anti-MHC-IIB (C-term) pAb (third and fifth panels), and anti-α-tubulin mAb (bottom panel). The signals of GFP-rod fragments (second panel) and endogenous MHC-IIA (forth panel) were detected simultaneously on the same immunoblot. The signals of GFP-rod fragments (third panel) and endogenous MHC-IIB (fifth panel) were detected simultaneously on the same immunoblot. α-tubulin was used as a loading control.

ARF296exN and ARF296exC were increased from that of original ARF296. In this case also, C-63 substitution was more effective. Interestingly, ARF296exNC, in which both regions were substituted, gained higher ability than the chimeras with substitution of only one side. Because the expression levels were almost the same among these fragments and significantly higher than that of endogenous MHC-IIB (Figure 4L), the difference of the effect would reflect the properties of each fragment. Time-lapse analysis revealed that the behaviors of GFP-ARF296exNC–expressing cells were quite similar to the GFP-BRF305–expressing cells (Supplementary Movie 4). These results indicate that N-57 and C-63 of BRF305 are both essential for the induction of aberrant cell shape; however, C-63 appears to be more important for this effect.

BRF305 Interacts with Endogenous Myosin IIB through Its N-57 and C-63

Next, we investigated whether the dominant negative effect of BRF305 is caused by the isoform-specific interaction of the exogenous rod fragment and endogenous myosin IIB. Immunoprecipitation of endogenous myosin IIB followed by immunoblotting with the anti-GFP antibodies revealed that GFP-BRF305 but not GFP-ARF296 coprecipitated with endogenous myosin IIB from extracts of the cells expressing each fragment (Figure 5). GFP-ARF296exNC also coprecipitated with endogenous myosin IIB (Figure 5). These results demonstrate that BRF305 interacts with endogenous myosin IIB in an isoform-specific manner and that the N-57 and C-63 of BRF305 are essential for this interaction. The mutant BRF305-m3 with defect in assembly did not coprecipitate with endogenous myosin IIB (Figure 5), indicating that the assembling ability of the rod fragment is necessary for the interaction as expected. These results support the idea that the induction of unstable cell shape is caused by the isoform-specific interaction of BRF305 with endogenous myosin IIB, and the N-57 and C-63 of BRF305, as well as its assembling ability, are essential for the induction.

Cortical Actin Cytoskeleton Including Myosin IIB Disappeared during Expression of BRF305 But Not ARF296

To explore the effect of exogenous expression of GFP-BRF305 on the actin cytoskeleton, we performed TRITC-phalloidin staining. In the control cells expressing GFP, F-actin appeared at the cell cortex as thick fiber structures and also in the cytoplasm as thin fiber structures (Figure 6, A–C). However, in GFP-BRF305–expressing cells, the well-defined actin fiber structures were not observed (Figure 6, D–F). On the other hand, in GFP-ARF296–expressing cells, the corti-

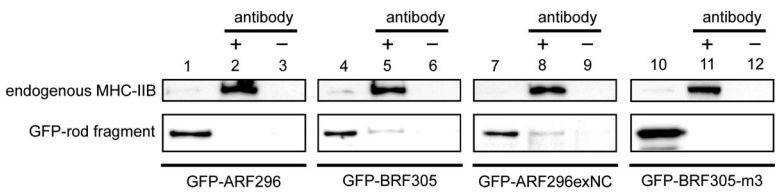

Figure 5. Coimmunoprecipitation of BRF305 and ARF296exNC with endogenous myosin IIB. Lysates from the cells, each expressing GFP-ARF296, GFP-BRF305, GFP-ARF296exNC, and GFP-BRF305-m3 (indicated below the panels), were incubated with anti-MHC-IIB (N-term) pAb to immunoprecipitate endogenous myosin IIB. The immunocomplexes were collected and analyzed by immunoblotting using anti-MHC-IIB (C-term) pAb and anti-GFP mAb for detecting endogenous MHC-IIB and each GFP-rod fragments, respectively. Top and bottom panels indicate endogenous MHC-IIB and GFP-rod fragments, respectively. Left lanes (1, 4, 7, and 10) of each panel are total lysates before immunoprecipitation. Center lanes (2, 5, 8, and 11) are samples of the immunocomplex. Right lanes (3, 6, 9, and 12) are samples without antibodies as negative control of immunoprecipitation.

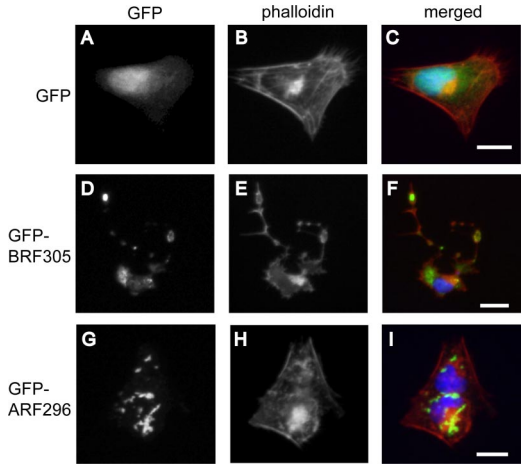

Figure 6. Disappearance of cortical actin fibers in GFP-BRF305–expressing cells, but not in GFP-ARF296–expressing cells. The cells expressing GFP as control (A–C), GFP-BRF305 (D–F), and GFP-ARF296 (G–I) were fixed and stained with TRITC-phalloidin (B, E, and H). (C, F, and I) Merged images of A and B, D and E, and G and H with DAPI staining (blue), respectively. The green and red colors indicate GFP and F-actin, respectively. Bar, 20 μm.

cal actin fiber structures remained but the cytoplasmic thin structures disappeared (Figure 6, G–I). All cells including control cells showed a structure stained with TRITC-phalloidin at perinuclear region. This undefined structure was often observed in MRC-5 SV1 TG1 cells. We assume this structure might be Golgi complex (Egea *et al.*, 2006). Next, we performed immunostaining of MHC-IIB to see endogenous myosin IIB localization in the rods expressing cells. In the control cells, myosin IIB localized strongly at the cell cortex except at the corners (Figure 7, A–C). Although the cortical localization of endogenous myosin IIB was reduced in GFP-BRF305–expressing cells (Figure 7, D–F), this still remained in GFP-ARF296–expressing cells (Figure 7, G–I). These results demonstrate that the cortical actin cytoskeleton including myosin IIB is reduced by the exogenous expression of BRF305 but not ARF296. This suggests that cells missing functional myosin IIB from the cell cortex could not maintain the actin cytoskeleton there and consequently induce the aberrant cell shape.

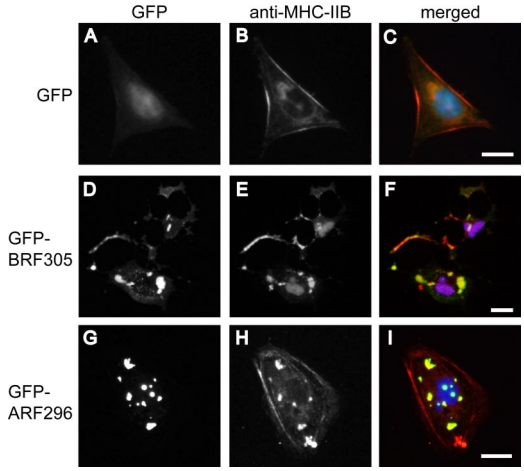

Figure 7. Myosin IIB remained at the cell cortex in GFP-ARF296–expressing cells. The cells expressing GFP as control (A–C), GFP-BRF305 (D–F), and GFP-ARF296 (G–I) were fixed and stained with anti-MHC-IIB pAb followed by detection with Cy3-labeled anti-rabbit IgG antibody (B, E, and H). Anti-MHC-IIB (C-term) pAb were used for GFP- and GFP-ARF296–transfected cells (B and H). Anti-MHC-IIB (N-term) pAb was used for GFP-BRF305 transfected cells (E) to distinguish between BRF305 and endogenous myosin IIB. (C, F, and I) Merged images of A and B, D and E, and G and H with DAPI staining (blue), respectively. The green and red colors indicate GFP and endogenous myosin IIB, respectively. Bar, 20 μm.

DISCUSSION

To clarify the role of vertebrate nonmuscle myosin II in cell motile processes, functional knockdown assays have been carried out, such as microinjection of antibodies against myosin II to a cell (Höner *et al.*, 1988; Zurek *et al.*, 1990). These studies demonstrated that myosin II molecules are involved in maintaining the cell shape in addition to changing cell shape such as cytokinesis. Recently, studies on the treatment of cells with blebbistatin, a specific inhibitor of nonmuscle myosin II ATPase activity, reconfirmed the function of myosin II (Straight *et al.*, 2003; Niggli *et al.*, 2006) and also revealed new aspects of the function (Rosenblatt *et al.*, 2004; Ryu *et al.*, 2006). However, these techniques cannot distinguish the function of each myosin II isoform.

Recently, information concerning the specific functions of myosin IIB have been increased by the studies of cells isolated from MHC-IIB knockout mice or small interfering RNA (siRNA)-treated cells. MHC-IIB$^{-/-}$ neurons appeared to have abnormal shapes and motile growth cones (Brown and Bridgman, 2003). MHC-IIB$^{-/-}$ fibroblasts demonstrated instability of cell shape and direction of migration (Lo *et al.*, 2004) and decreased ability to contract 3D collagen gel (Meshel *et al.*, 2005). A defect in cytokinesis was observed in MHC-IIB$^{-/-}$ cardiac myocyte (Takeda *et al.*, 2003) and siRNA-treated COS-7 cells (Bao *et al.*, 2005), possibly because myosin IIA is absent in these cells. Abnormal morphology of dendritic spines was also observed in siRNA-treated neurons (Ryu *et al.*, 2006).

In this article, we showed that exogenous expression of BRF305 in the MRC-5 SV1 TG1 cells induced an unstable cell shape similar to MHC-IIB$^{-/-}$ fibroblasts. We demonstrated this dominant negative effect was likely caused in an isoform-specific manner. Moreover, two regions, N-57 (Leu 1672-Leu 1728) and C-63 (Asn 1914-Glu 1976) of BRF305, were important for this effect.

How BRF305 can inhibit the endogenous myosin IIB function in the cell and then induce an abnormality in the cell motile processes? Formation of bipolar filament is necessary for myosin II to function, and the dynamic filament assembly-disassembly transition is particularly important in nonmuscle cells. In practice, dynamic exchange of myosin II in the cell cortex was observed in living *Dictyostelium* cells, and the mutants having a defect in the assembly-disassembly transition could not achieve this dynamic exchange process (Yumura, 2001). We showed here that overexpression of the fragments being able to interact with endogenous myosin IIB could induce the aberrant phenotype (Figures 2, 4, and 5). These results can be understood as follows: BRF305 could interact with a monomer of endogenous myosin IIB that dissociated from the filament during the dynamic assembly-disassembly process, and the resulting myosin IIB-BRF305 complex could not reassemble into normal filaments under the experimental conditions with high expression levels of exogenous BRF305. As a result, functional myosin IIB filaments were lost.

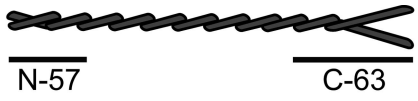

A

```
MHC-IIB 1672 FAQSKESEKKLKSLEAEILQLQEELASSERARRHAEQERDELADEITNSASGKSALL 1728
             ** ** ****** ***  *******  *** * * ********** **       *
MHC-IIA 1666 LAQAKENEKKLKSMEAEMIQLQEELAAAERAKRQAQQERDELADEIANSSGKGALAL 1722
```

B

```
MHC-IIB 1914 NEGLSREVSTLKNRLRRGGPISFSSSRSGRRQLHLEGASLELSDDDTESKTSDVNETQPPQSE 1976
                  **** *** ****         * *              *
MHC-IIA 1908 ADAMNREVSSLKNKLRRGDLPFVVPRRMARKGAGDGSDEEVDGKADGAEAKPAE 1961
```

Figure 8. Alignment of the amino acid sequences of N-57 and C-63 of BRF305 with corresponding region of ARF296. Schematic illustration represents the portions of N-57 and C-63 region in the rod fragment. (A) N-57 of BRF305 and corresponding ARF296. (B) C-63 of BRF305 and corresponding ARF296. Asterisks indicate identical amino acid residues.

The next question is why the inhibition of endogenous myosin IIB function induces instability of cell shape. It has been demonstrated that myosin IIB tended to localize in restricted regions in a cell compared with myosin IIA (Maupin *et al.*, 1994; Rochlin *et al.*, 1995; Saitoh *et al.*, 2001; Kolega, 2003; Lo *et al.*, 2004). For example, in migrating endothelial cells, myosin IIA biased toward the front, whereas myosin IIB accumulated in the rear (Kolega, 2003). In migrating fibroblasts, myosin IIA localized to the lamella and throughout the posterior region, whereas myosin IIB is localized to the posterior region, especially at the lateral cell cortex (Saitoh *et al.*, 2001). From these observations and the unstable phenotype of MHC-IIB$^{-/-}$ fibroblasts (Lo *et al.*, 2004), it has been suggested that myosin IIB is involved in the maintenance of cell shape and polarity to prevent undesirable protrusion in posterior region. We showed here, that myosin IIB was preferentially localized at the cell cortex with actin fibers in MRC-5 SV1 TG1 cells. This localization still remained in the ARF296-expressing cells, but was not maintained in the BRF305-expressing cells (Figures 6 and 7). Taken together, we speculate that a cell losing functional myosin IIB at the cell cortex cannot maintain the actin network, resulting in the induction of an unstable phenotype.

The present results of the exogenous expression of the deletion mutants (Figure 3) and of the chimeric fragments (Figure 4) revealed that two regions, N-57 and C-63 of BRF305, were important for the induction of aberrant cell shape. In other words, these two regions would be involved in self-recognition of myosin IIB to form homo-filament in the cell. The results indicated that C-63 was more effective for this recognition than N-57 (Figure 4).

It should be noted that C-63 includes the nonhelical tailpiece where the differences in primary structures of isoforms are clustered (Figure 8). Moreover, a few phosphorylation sites have been identified within this C-terminal region (Murakami *et al.*, 1990, 1998; Conti *et al.*, 1991; Even-Faitelson and Ravid, 2006; Rosenberg and Ravid, 2006). Phosphorylation within this region by PKC isoforms reduced the assembling ability of myosin IIB (Murakami *et al.*, 1995; Even-Faitelson and Ravid, 2006; Rosenberg and Ravid, 2006). On the other hand, it was demonstrated that the assembly of myosin IIA was also regulated through the C-terminal region. In vitro studies revealed that Mts1, a member of S100 family of Ca^{2+}-binding proteins, binds to this region of myosin IIA and keeps the myosin IIA in a monomer state (Murakami *et al.*, 2000; Li *et al.*, 2003) and also inhibits the phosphorylation within this region (Kriajevska *et al.*, 1998; Dulyaninova *et al.*, 2005). It has been suggested that the assembly of each isoform is regulated by a distinct mechanism through modification of the C-terminal end region, that is, phosphorylation by protein kinase C for myosin IIB and Mts1 binding for myosin IIA, and this distinction contributes to the homo-filament formation (Murakami *et al.*, 2000). Because the 72-kDa rod fragment of myosin IIB was phosphorylated in the cell (Ben-Ya'acov and Ravid, 2003), it is possible that the rod fragments used in this study were modified by phosphorylation or by binding of other protein such as Mts1 in the cell. This modification could be involved in self-recognition of the rod fragments expressed in the cell.

The role of N-57 in self-recognition can be explained by the molecular packing model proposed previously (Nakasawa *et al.*, 2005). The proposed antiparallel packing model of BRF248, though it lacks the N-57, allowed us to predict that N-57 in one fragment may be the interaction site for C-63 in the partner fragment. Although the primary structure of the N-57 region is not so different between myosin IIB and myosin IIA (Figure 8), our results (Figures 4 and 5) imply that the small difference could be important for self-recognition. The interaction between N-57 and C-63 may play a key role in self-recognition.

MHC-IIB-specific siRNA-treated MRC-5 SV1 TG1 cells showed aberrant cell shape like BRF305-expressing cells, but the percentage of the cells exhibiting the aberrant shape and their degrees of aberrancy were lower than those of BRF305-expressing cells (Supplementary Figure S2). Two different explanations could account for this result. 1) The few myosin IIB remaining in siRNA-treated cells (12.8 $\pm$ 3.3%) could work to maintain cell shape partially. 2) In BRF305-expressing cells, besides interacting with the endogenous myosin IIB (Figure 5), BRF305 may sequester some proteins maintaining cell shape. If such protein exists, it could interact with myosin IIB filament at N-57 and C-63, because ARF296exNC induced the aberrant cell shape but BRF305-m3 did not.

A part of endogenous myosin IIB existed in the aggregates observed in both BRF305- and ARF296-expressing cells (Figure 7, D–I). The exogenous expression of rod fragments could induce the collapse of actin cytoskeleton in isoform-specific manner, and then some dispersed components might aggregate randomly without distinction of isoforms. Because the immunoprecipitation assay revealed that endogenous myosin IIB did not interact with ARF296 (Figure 5), we assume that direct interaction between exogenous rod fragments and endogenous myosin II isoforms might not occur in these aggregates.

It was demonstrated that expression of a truncated fragment of myosin IIA, lacking N-terminal 592 amino acid residues, induced cell rounding in a HeLa cell line (Clontech Tet-off system: which does not express MHC-IIB) because of the disruption of focal adhesions (Wei and Adelstein, 2000). We could not detect a remarkable defect in cell shape of MRC-5 SV1 TG1 cells by the expression of ARF296 (Figure 3). However, we suppose that the expression of ARF296 showed some inhibitory effect, because we observed the disruption of actin thin-fiber structures in the cytoplasm (Figure 6). It is thus possible that the disruption exerts some cell motile processes, which we have not noticed yet. The lack of the clear effects of myosin IIA inhibition in MRC-5 SV1 TG1 cells might be explained as following reasons. 1) The relative expression level of ARF296 against endogenous myosin IIA is not enough to show its inhibitory effect completely in this cell line. We estimated that the relative expression level of GFP-ARF296 was approximately three times higher than that of endogenous MHC-IIA. On the other hand, the relative expression level of GFP-BRF305

against the endogenous MHC-IIB was estimated ~90 times (Figure 3 and Supplementary Figure S1). 2) Differed from the HeLa cell line (Clontech Tet-off system), MRC-5 SV1 TG1 cells express MHC-IIB as well as MHC-IIA. We have treated MRC-5 SV1 TG1 cells with blebbistatin to inhibit myosin IIA besides myosin IIB and observed resulting morphological phenotypes. The blebbistatin-treated cells showed aberrant cell shape similar to the BRF305-expressing cells (Supplementary Figure S3). We cannot observe another defect on cell shape; it is thus speculated that myosin IIB makes a large contribution to maintain cell shape in this cell line. Recently by Betapudi *et al.* (2006), and during the revision of this manuscript (Sandquist *et al.*, 2006; Cai *et al.*, 2006), it was reported that depletion of myosin II isoforms by specific siRNA-treatments caused cells to alter their speed of migration and spreading. However, the effects of depletion of each isoform are not completely the same among the reports, possibly because of the difference of the used cell species. It is necessary to study the function of each isoform considering their expression levels in different cell types. We roughly estimated that the relative expression level of MHC-IIA was 15 times higher than that of MHC-IIB in MRC-5 SV1 TG1 cells by immunoprecipitation of each isoform with specific antibodies, followed by immunoblotting with a pan-myosin antibody (Supplementary Figure S1). Further investigation using this cell and also other cells, in which the relative expression level of MHC-IIA is lower than in this cell, might reveal an obvious dominant negative effect of ARF296.

In this work, we demonstrated that N-57 and C-63 regions of BRF305 are involved in self-recognition of myosin IIB by using the cytoplasm as a "living test tube" to study protein interactions and their effects on cell behavior. Further studies on the role of these regions would clarify the molecular mechanisms for homo-assembling processes and also for the isoform-specific cellular functions.

ACKNOWLEDGMENTS

We are grateful to Dr. Robert S. Adelstein (NHLBI, National Institutes of Health [NIH], Bethesda, MD) for helpful discussion and critical reading of the manuscript. We are also grateful to Dr. Mary Anne Conti (NHLBI, NIH) for helpful advice on immunofluorescence. We thank Dr. Hisashi Haga (Division of Biological Sciences, Graduate School of Science, Hokkaido University, Sapporo, Japan) for the helpful advice on time-lapse microscopy. We also thank Shuhei Takemura and Masanao Ashio for technical assistance. This work was supported in part by Grants-in-Aid for Scientific Research 18570144 (M.T.) from the Japan Society for the Promotion of Science.

REFERENCES

Bao, J., Jana, S. S., and Adelstein, R. S. (2005). Vertebrate nonmuscle myosin II isoforms rescue small interfering RNA-induced defects in COS-7 cell cytokinesis. J. Biol. Chem. *280*, 19594–19599.

Ben-Ya'acov, A., and Ravid, S. (2003). Epidermal growth factor-mediated transient phosphorylation and membrane localization of myosin II-B are required for efficient chemotaxis. J. Biol. Chem. *278*, 40032–40040.

Berg, J. S., Powell, B. C., and Cheney, R. E. (2001). A millennial myosin census. Mol. Biol. Cell *12*, 780–794.

Betapudi, V., Licate, L. S., and Egelhoff, T. T. (2006). Distinct roles of nonmuscle myosin II isoforms in the regulation of MDA-MB-231 breast cancer cell spreading and migration. Cancer Res. *66*, 4725–4733.

Brown, M. E., and Bridgman, P. C. (2003). Retrograde flow rate is increased in growth cones from myosin IIB knockout mice. J. Cell Sci. *116*, 1087–1094.

Cai, Y. *et al.* (2006). Nonmuscle myosin IIA-dependent force inhibits cell spreading and drives F-actin flow. Biophys. J. *91*, 3907–3920.

Conti, M. A., Sellers, J. R., and Adelstein, R. S. (1991). Identification of the serine residue phosphorylated by protein kinase C in vertebrate nonmuscle myosin heavy chains. Biochemistry *30*, 966–970.

Conti, M. A., Even-Ram, S., Liu, C., Yamada, K. M., and Adelstein, R. S. (2004). Defects in cell adhesion and the visceral endoderm following ablation of nonmuscle myosin heavy chain II-A in mice. J. Biol. Chem. *279*, 41263–41266.

Craig, R., and Woodhead, J. L. (2006). Structure and function of myosin filaments. Curr. Opin. Struct. Biol. *16*, 204–212.

Dulyaninova, N. G., Malashkevich, V. N., Almo, S. C., and Bresnick, A. R. (2005). Regulation of myosin IIA assembly and Mts1 binding by heavy chain phosphorylation. Biochemistry *44*, 6867–6876.

Egea, G., Lázaro-Diéquez, F., and Viella, M. (2006). Actin dynamics at the Golgi complex in mammalian cells. Curr. Opin. Cell Biol. *18*, 168–175.

Even-Faitelson, L., and Ravid, S. (2006). PAK1 and aPKCζ regulate myosin II-B phosphorylation: a novel signaling pathway regulating filament assembly. Mol. Biol. Cell *17*, 2869–2881.

Geiser, M., Cèbe, R., Drewello, D., and Schmitz, R. (2001). Integration of PCR fragments at any specific site within cloning vectors without the use of restriction enzymes and DNA ligase. Biotechniques *31*, 88–92.

Golomb, E., Ma, X., Jana, S. S., Preston, Y. A., Kawamoto, S., Shoham, N. G., Goldin, E., Conti, M. A., Sellers, J. R., and Adelstein, R. S. (2004). Identification and characterization of nonmuscle myosin II-C, a new member of the myosin II family. J. Biol. Chem. *279*, 2800–2808.

Hodge, T. P., Cross, R., and Kendrick-Jones, J. (1992). Role of the COOH-terminal nonhelical tailpiece in the assembly of a vertebrate nonmuscle myosin rod. J. Cell Biol. *118*, 1085–1095.

Höner, B., Citi, S., Kendrick-Jones, J., and Jockusch, B. M. (1988). Modulation of cellular morphology and locomotory activity by antibodies against myosin. J. Cell Biol. *107*, 2181–2189.

Kelley, C. A., Sellers, J. R., Gard, D. L., Bui, D., Adelstein, R. S., and Baines, I. C. (1996). *Xenopus* nonmuscle myosin heavy chain isoforms have different subcellular localizations and enzymatic activities. J. Cell Biol. *134*, 675–687.

Kolega, J. (1998). Cytoplasmic dynamics of myosin IIA and IIB: spatial 'sorting' of isoforms in locomoting cells. J. Cell Sci. *111*, 2085–2095.

Kolega, J. (2003). Asymmetric distribution of myosin IIB in migrating endothelial cells is regulated by a rho-dependent kinase and contributes to tail retraction. Mol. Biol. Cell *14*, 4745–4757.

Kriajevska, M., Tarabykina, S., Bronstein, I., Maitland, N., Lomonosov, M., Hansen, K., Georgiev, G., and Lukanidin, E. (1998). Metastasis-associated Mts1 (S100A4) protein modulates protein kinase C phosphorylation of the heavy chain of nonmuscle myosin. J. Biol. Chem. *273*, 9852–9856.

Laemmli, U. K. (1970). Cleavage of structural proteins during the assembly of the head of bacteriophage T4. Nature *227*, 680–685.

Lauffenburger, D. A., and Horwitz, A. F. (1996). Cell migration: a physically integrated molecular process. Cell *84*, 359–369.

Li, Z. H., Spektor, A., Varlamova, O., and Bresnick, A. R. (2003). Mts1 regulates the assembly of nonmuscle myosin-IIA. Biochemistry *42*, 14258–14266.

Lo, C. M., Buxton, D. B., Chua, G.C.H., Dembo, M., Adelstein, R. S., and Wang, Y. L. (2004). Nonmuscle myosin IIB is involved in the guidance of fibroblast migration. Mol. Biol. Cell *15*, 982–989.

Matsumura, F. (2005). Regulation of myosin II during cytokinesis in higher eukaryotes. Trends Cell Biol. *15*, 371–377.

Maupin, P., Phillips, C. L., Adelstein, R. S., and Pollard, T. D. (1994). Differential localization of myosin-II isozymes in human cultured cells and blood cells. J. Cell Sci. *107*, 3077–3090.

McLachlan, A. D. (1984). Structural implications of the myosin amino acid sequence. Annu. Rev. Biophys. Bioeng. *13*, 167–189.

Meshel, A. S., Wei, Q., Adelstein, R. S., and Sheetz, M. P. (2005). Basic mechanism of three-dimensional collagen fibre transport by fibroblasts. Nat. Cell Biol. *7*, 157–164.

Mitchison, T. J., and Cramer, L. P. (1996). Actin-based cell motility and cell locomotion. Cell *84*, 371–379.

Murakami, N., Healy-Louie, G., and Elzinga, M. (1990). Amino acid sequence around the serine phosphorylated by casein kinase II in brain myosin heavy chain. J. Biol. Chem. *265*, 1041–1047.

Murakami, N., Singh, S. S., Chauhan, V.P.S., and Elzinga, M. (1995). Phospholipid binding, phosphorylation by protein kinase C, and filament assembly of the COOH terminal heavy chain fragments of nonmuscle myosin II isoforms MIIA and MIIB. Biochemistry *34*, 16046–16055.

Murakami, N., Chauhan, V.P.S., and Elzinga, M. (1998). Two nonmuscle myosin II heavy chain isoforms expressed in rabbit brains: filament forming properties, the effects of phosphorylation by protein kinase C and casein

kinase II, and location of the phosphorylation sites. Biochemistry *37*, 1989–2003.

Murakami, N., Kotula, L., and Hwang, Y. W. (2000). Two distinct mechanisms for regulation of nonmuscle myosin assembly via the heavy chain: phosphorylation for MIIB and Mts1 binding for MIIA. Biochemistry *39*, 11441–11451.

Nakasawa, T., Takahashi, M., Matsuzawa, F., Aikawa, S., Togashi, Y., Saitoh, T., Yamagishi, A., and Yazawa, M. (2005). Critical regions for assembly of vertebrate nonmuscle myosin II. Biochemistry *44*, 174–183.

Niggli, V., Schmid, M., and Nievergelt, A. (2006). Differential roles of Rho-kinase and myosin light chain kinase in regulating shape, adhesion, and migration of HT1080 fibrosarcoma cells. Biochem. Biophys. Res. Commun. *343*, 602–608.

Robinson, D. N., and Spudich, J. A. (2004). Mechanics and regulation of cytokinesis. Curr. Opin. Cell Biol. *16*, 182–188.

Rochlin, M. W., Itoh, K., Adelstein, R. S., and Bridgman, P. C. (1995). Localization of myosin II A and B isoforms in cultured neurons. J. Cell Sci. *108*, 3661–3670.

Rosenberg, M., and Ravid, S. (2006). Protein kinase Cγ regulates myosin IIB phosphorylation, cellular localization, and filament assembly. Mol. Biol. Cell *17*, 1364–1374.

Rosenblatt, J., Cramer, L. P., Baum, B., and McGee, K. M. (2004). Myosin II-dependent cortical movement is required for centrosome separation and positioning during mitotic spindle assembly. Cell *117*, 361–372.

Ryu, J., Liu, L., Wong, T. P., Wu, D. C., Burette, A., Weinberg, R., Wang, Y. T., and Sheng, M. (2006). A critical role for myosin IIB in dendritic spine morphology and synaptic function. Neuron *49*, 175–182.

Saitoh, T., Takemura, S., Ueda, K., Hosoya, H., Nagayama, M., Haga, H., Kawabata, K., Yamagishi, A., and Takahashi, M. (2001). Differential localization of non-muscle myosin II isoforms and phosphorylated regulatory light chain in human MRC-5 fibroblasts. FEBS Lett. *509*, 365–369.

Sandquist, J. C., Swenson, K. I., DeMali, K. A., Burridge, K., and Means, A. R. (2006). Rho kinase differentially regulates phosphorylation of nonmuscle myosin II isoforms A and B during cell rounding and migration. J. Biol. Chem. *281*, 35873–35883.

Sellers, J. R. (1999). Myosins, 2nd Ed., Oxford, UK: Oxford University Press.

Sohn, R. L., Vikstrom, K. L., Strauss, M., Cohen, C., Szent-Gyorgyi, A. G., and Leinwand, L. A. (1997). A 29 residue region of the sarcomeric myosin rod is necessary for filament formation. J. Mol. Biol. *266*, 317–330.

Straight, A. F., Cheung, A., Limouze, J., Chen, I., Westwood, N. J., Sellers, J. R., and Mitchison, T. J. (2003). Dissecting temporal and spatial control of cytokinesis with a myosin II inhibitor. Science *299*, 1743–1747.

Takahashi, M., Hirano, T., Uchida, K., and Yamagishi, A. (1999). Developmental regulated expression of a nonmuscle myosin heavy chain IIB inserted isoform in rat brain. Biochem. Biophys. Res. Commun. *259*, 29–33.

Takeda, K., Kishi, H., Ma, X., Yu, Z. X., and Adelstein, R. S. (2003). Ablation and mutation of nonmuscle myosin heavy chain II-B results in a defect in cardiac myocyte cytokinesis. Circ. Res. *93*, 330–337.

Tullio, A. N., Accili, D., Ferrans, V. J., Yu, Z. X., Takeda, K., Grinberg, A., Westphal, H., Preston, Y. A., and Adelstein, R. S. (1997). Nonmuscle myosin II-B is required for normal development of the mouse heart. Proc. Natl. Acad. Sci. USA *94*, 12407–12412.

Wei, Q., and Adelstein, R. S. (2000). Conditional expression of a truncated fragment of nonmuscle myosin II-A alters cell shape but not cytokinesis in HeLa cells. Mol. Biol. Cell *11*, 3617–3627.

Yumura, S. (2001). Myosin II dynamics and cortical flow during contractile ring formation in *Dictyostelium* cells. J. Cell Biol. *154*, 137–145.

Zurek, B., Sanger, J. M., Sanger, J. W., and Jockusch, B. M. (1990). Differential effects of myosin-antibody complexes on contractile rings and circumferential belts in epithelial cells. J. Cell Sci. *97*, 297–306.